# Corrosion resistance of tungsten and nickel in molten eutectic mixture LiF-NaF-KF

**Marta Ambrová, Vladimír Danielik**

[a] *Institute of Inorganic Chemistry, Technology and Materials, Faculty of Chemical and Food Technology, Slovak University of Technology, Radlinského 9, SK-812 37, Bratislava, Slovakia*
*marta.ambrova@stuba.sk*

**Abstract:** Corrosion resistance of tungsten and nickel in molten eutectic mixture LiF-NaF-KF was investigated by measurement of polarization resistance and chronopotentiometry. Results obtained by both methods were compared by digital simulation of diffusion of corrosion products. All measurements were carried out at the temperature of 680 °C in inert argon atmosphere and in oxidation air atmosphere. Surface of the metal samples after measurements was investigated by scanning electron microscope and X-ray microanalysis that was, together with X-ray diffraction analysis, used for the identification of corrosion products.

**Keywords:** corrosion of metals, chronopotentiometry, polarization resistance

## Introduction

Molten salts are mainly used for the electrowinning of light metals and chemical or electrochemical deposition of metals and metalloids (Büchel et al. 2000). Their usage in the other industrial areas also acquires on importance. The most interesting seems to be application of molten salts as a heat transfer medium for a new generation of nuclear reactors (Generation IV) as well as for the spent nuclear fuel treatment. This, however, requires usage of highly corrosion resistant materials. For the development of such materials, a study of the corrosion of basic metals and knowledge of its mechanism is inevitable zero step.

In this work, corrosion resistance of tungsten and nickel in the molten eutectic mixture LiF-NaF-KF at the temperature of 680 °C in inert argon atmosphere and in oxidation air atmosphere was investigated. The use of the eutectic mixture LiF-NaF-KF is expected in the secondary (heat transfer) circuit of nuclear reactors operating on the base of molten salts. Selected metals are considered as major components of highly corrosion resistant materials. It is not expected that the molten salts could be in direct contact with the air during operation. However, some risk poses an equipment failure or a purity of molten salts. Therefore, the corrosion resistance of metal samples was tested also under oxidation conditions, i.e. in the air atmosphere.

## Experimental

### *Methodology*

*Polarization resistance*

Measurement of polarization resistance is widely used method in the corrosion monitoring (Joska and Novák 2001). Polarization resistance of material $R_p$ is defined as a slope of the potential-current density curve at the free corrosion potential. In general,

$$j_{cor} = \frac{B}{R_p} \tag{1}$$

$$B = \frac{b_a \cdot b_c}{2.303 \cdot (b_a + b_c)} \tag{2}$$

$$R_p = \frac{\Delta E}{\Delta j} \tag{3}$$

where $j_{cor}$ is the corrosion current density; $R_p$ is the polarization resistance evaluated close to the corrosion potential ($\Delta E \to 0$), $b_a$ and $b_c$ are the slopes of Taffel dependence $\log j = f(\Delta E)$ in anodic and cathodic area, respectively, $\Delta E$ is the difference between measured and corrosion potential and $j$ is the current density at $\Delta E$. Corrosion rate is then calculated according to Faraday's laws (Koryta, 1980).

*Chronopotentiometry*

Chronopotentiometry is the electrochemical method based on the measurement of potential of the working electrode (in this case tested metal sample) as a function of time, when a constant current passes through the system (Bard and Faulkner 2001). The electrode potential changes as a result of the electrochemical consumption of electroactive species at the surface of the electrode. When the surface concentration of the electroactive species drops to zero, potential of the electrode changes rapidly. Time that elapses from the beginning of electrolysis to the abrupt change of potential is called the transition time $\tau$. When the rate of the electrochemical process is controlled only by diffusion of the electroactive species, the process is described by Sand's equation (Sand 1901),

$$\tau^{1/2} = \frac{nFc^0\pi^{1/2}D^{1/2}}{2|j|} \quad (4)$$

where $\tau$ is the transition time, $n$ is the number of exchanged electrons, $F$ is Faraday's constant ($F$ = 96485.3 C·mol$^{-1}$), $c^0$ is the molar concentration, $D$ is the diffusion coefficient and $j$ is the current density. Given equation represents relationship between transition time and current density, molar concentration and diffusion coefficient of electroactive species. Since the diffusion coefficient can be determined independently for known molar concentration of electroactive species, the chronopotentiometry can be used as an electroanalytical method.

***Working procedure***

Analytical grade chemicals LiF (Suprapur, Merck, Germany), NaF (Merck, Germany), KF (Lachema, Czech Republic) and $NiF_2$ (Aldrich, USA) were used. They were dried in a closed furnace heated up to 600 °C for 4 hours. Since KF is hygroscopic, it was dried by $P_2O_5$ in a vacuum dryer for 7 days, instead. Tungsten and nickel wires, thickness of 1 mm and purity of 99.99 %, were supplied by Aldrich, USA.

Polarization resistance and chronopotentiometric studies were performed with the use of an Autolab PGSTAT20 potentiostat/galvanostat (ECO Chemie, The Netherlands) controlled by a computer. The cell consisted of a graphite crucible which, at the same time, served as the counter electrode. Metal sample (tungsten or nickel) was used as working electrode and Ni/Ni$^{2+}$ electrode as reference electrode. The contact area between metal sample and melt was determined after each experiment by measuring the immersion depth in the bath.

A graphite crucible containing 130 g of dried eutectic mixture (46.5 mole % LiF, 11.5 mole % NaF and 42.0 mole % KF) was placed either in a closed laboratory furnace under inert argon atmosphere, or in an open furnace that provided contact with the air. Prior to furnace inlet, argon (99.99 %, Messer Tatragas) was dried by bubbling through sulphuric acid, and traces of oxygen were removed on copper cuttings heated to 350 °C. After melting, the molten mixture was kept at constant temperature of (680 ± 2) °C, controlled by a Pt–Pt10Rh thermocouple. After an immersion of metal sample, the measurements were performed at approximately equal intervals. The dependence $I = f(E)$ was measured in the potential range ±200 mV from the corrosion potential $E_{cor}$ with polarization rate 0.001 V·s$^{-1}$.

Surface of samples after corrosion was analysed by scanning electron microscope (Zeiss EVO 40, REM TESLA-BS 300, Slovakia) and X-ray microanalysis (EDX, probe EPMA JEOL JXA-840 A, Japan) that was, together with X-ray diffraction analysis (STOE stadi P, Bruker D8 Advance Super Speed, Germany), also used for the identification of corrosion products.

## Results and Discussion

In Fig. 1, comparison of the time dependence of corrosion current density obtained during corrosion of tungsten in inert argon atmosphere and oxidation air atmosphere is shown. As can be seen from figure, corrosion rate has the same trend in both cases, although it is higher in the presence of air (oxygen) than in its absence. From the final stage of corrosion measurement it can be assumed that the corrosion rate will slightly decrease to some constant value. Overall change of thickness of tungsten (calculated under assumption that the average number of electrons exchanged at the electrochemical process is 3) in this stage of corrosion corresponds to the value of $8.1 \cdot 10^{-1}$ cm·r$^{-1}$ and $9.4 \cdot 10^{-1}$ cm·r$^{-1}$ in the absence and presence of air, respectively. It can be concluded that presence of air does not significantly influence corrosion resistance of tungsten.

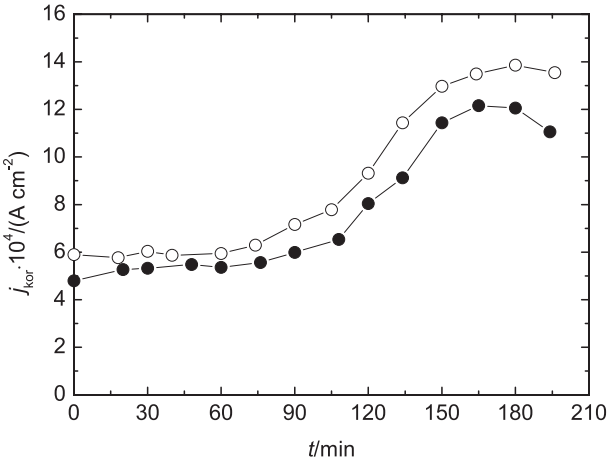


**Fig. 1.** Comparison of the corrosion current density obtained during corrosion of tungsten in argon atmosphere (●) and in air atmosphere (○).

In Fig. 2, surface of tungsten before and after corrosion in the absence and in the presence of air obtained by scanning electron microscope is shown. While the surface of tungsten has a uniform microstructure without any significant inhomogeneities (a typical texture is the result of grinding the electrode surface) before corrosion measurement, a rare occurrence of the areas with a new phase can be observed after corrosion measurement, the visible material contrast corresponds to the phase separation. After the corrosion measurement in

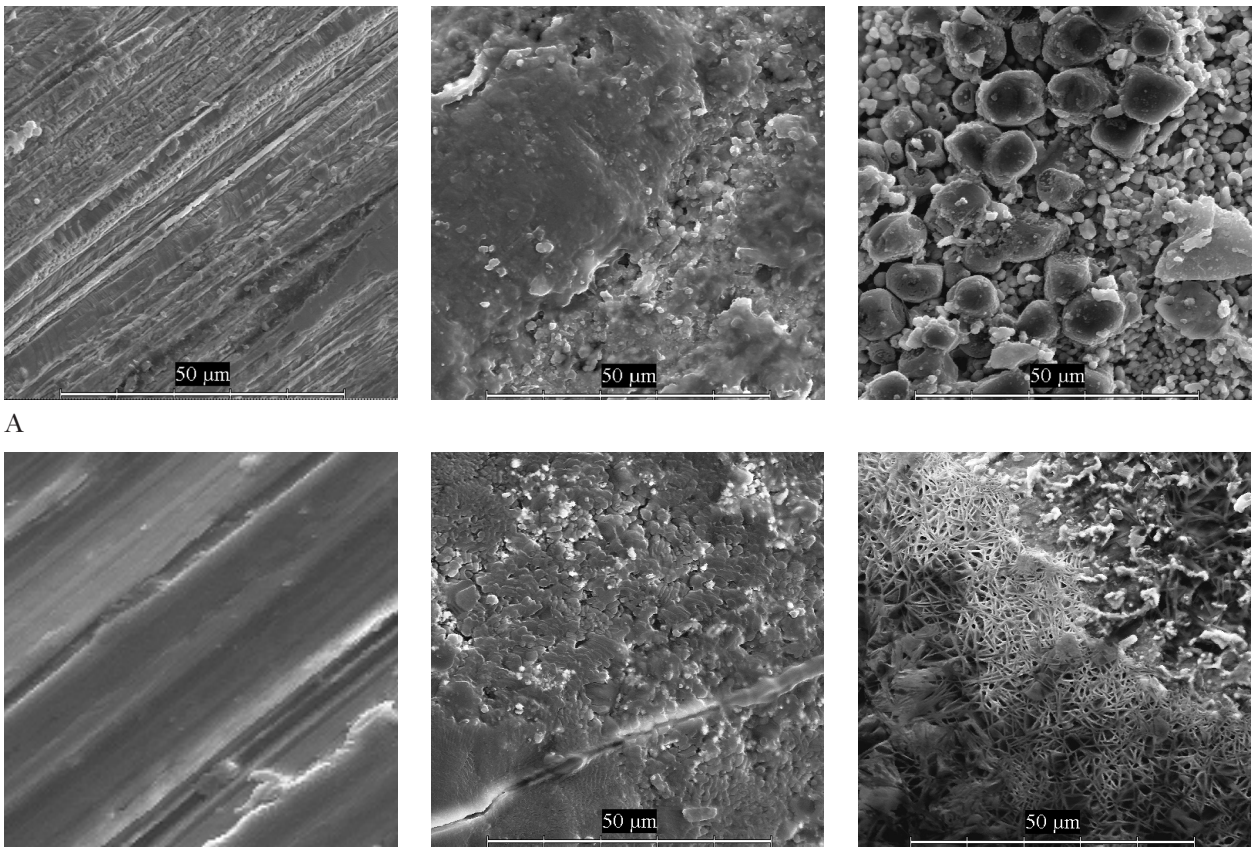


**Fig. 2.** Surface of tungsten (A) and nickel (B) before and after corrosion.

the presence of air, the surface becomes uniformly rugged, covered with a newly formed crystallic or granular layer.

In Table 1, composition of the corrosion products present on the surface of tungsten and in the solidified melt after corrosion measurements is given. As can be seen, no corrosion products were identified in the solidified melt after corrosion measurement performed in the absence of air. It can be assumed that corrosion products are only slightly soluble in the melt (below detection limit of X-ray diffraction analysis) and remain on the metal surface that partly inhibits corrosion process. On the other side, the presence of tungsten compounds in the solidified melt after corrosion measurement performed in the presence of air (oxygen) indicates that the formed tungstates are soluble in the melt (in the detection limits of X-ray diffraction analysis) that can support corrosion process. However, the other corrosion products, present on the surface of tungsten in the form of grains, can cause that the corrosion process is inhibited. This assumption can partly explain similar corrosion rates of tungsten in the absence and in the presence of air (oxygen).

In Fig. 3, comparison of the time dependence of corrosion current density obtained during corrosion of nickel in inert argon atmosphere and oxidation air atmosphere is shown.

As can be seen from figure, corrosion rate has the same trend in both cases. However, it is significantly

**Tab. 1.** Composition of the melt and surface of metal samples after corrosion.

| Sample | Composition of the melt | | Composition of the surface | |
|---|---|---|---|---|
| | in argon atm | in air atm | in argon atm | in air atm |
| tungsten | LiF, NaF, KF, $KF{\cdot}2H_2O$ | LiF, NaF, KF, $Na_{0.30}WO_3$, $KNa_3WO_5$, $K_6W_2O_9$, $K_2W_3O_{10}$ | W, probably fluorotungstate the type of $NaWF_6$ | W, $Na_3WO_3F_3$, $K_{0.39}Na_{0.27}WO_3$, $K_2W_8O_{20.8}$ |
| nickel | LiF, NaF, $NaNiO_2$, $NiF_2$ | LiF, NaF, KF, $KF_2 \cdot H_2O$ | Ni, $Li_2NiF_4$ | Ni, $LiNiO_2$ |

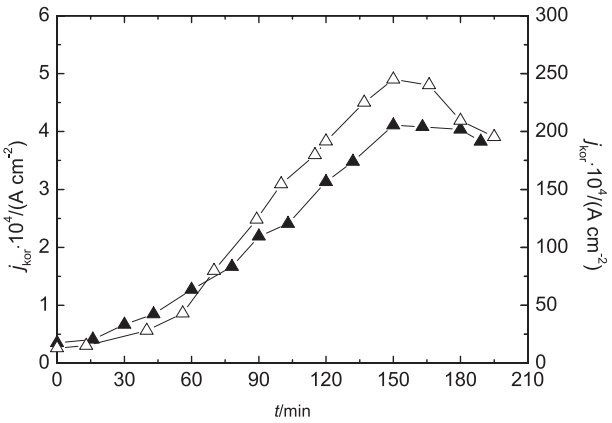


**Fig. 3.** Comparison of the corrosion current density obtained during corrosion of nickel in argon atmosphere (▲), in air atmosphere (△; right axis).

higher in the presence of air (oxygen) than in its absence. From the final stage of corrosion measurement it can be assumed that the corrosion rate will slightly decrease to some constant value. Overall change of thickness of nickel (calculated under assumption that the average number of electrons exchanged at the electrochemical process is 2) in this stage of corrosion corresponds to the value of $2.5 \cdot 10^{-1}$ cm·r$^{-1}$ and $144.3 \cdot 10^{-1}$ cm·r$^{-1}$ in the absence and presence of air, respectively. It can be concluded that the presence of air (oxygen) in molten eutectic LiF-NaF-KF significantly decreases corrosion resistance of nickel.

In Fig. 2, surface of nickel before and after corrosion in the absence and in the presence of air obtained by scanning electron microscope is shown. While the surface of nickel has a uniform microstructure without any significant inhomogeneities (a typical texture is the result of grinding the electrode surface) before corrosion measurement, the formation of cracks and a rare occurrence of the areas with a new phase (that can inhibit corrosion process) can be observed after corrosion measurement performed in the absence of air. Presence of nickel compounds in the solidified melt after corrosion measurement (see Table 1), indicates their solubility in the melt.

After corrosion measurement performed in the presence of air, the surface becomes significantly rugged even powdered, with uneven splinter of the recrystallized blocks of material (layers). Rugged (crystalline) areas, formed to the blocks, prevail in the structure, occasionally occur unrecrystallized areas with a new phase. It seems that the corrosion products of nickel are not soluble in the melt, in this case. However, they form layers that are cracked and non-adhesive to the surface. Thus passivation of the nickel surface does not occur and corrosion rate is rapidly higher than in the case of inert argon atmosphere.

In Figs. 4 and 5, comparison of the time dependence of corrosion current density obtained during corrosion of tungsten and nickel in inert argon and oxidation air atmosphere, respectively, is shown. As follows from figures, corrosion rate has similar trend in both cases. However, under inert argon atmosphere the more corrosion resistant metal is nickel and under oxidation air atmosphere the more corrosion resistant metal is tungsten.

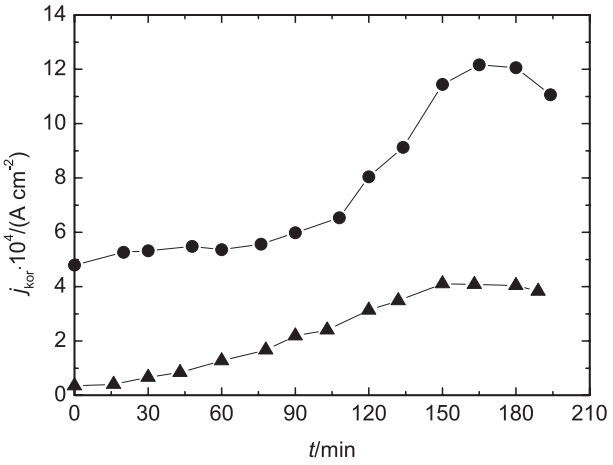


**Fig. 4.** Comparison of the corrosion current density obtained during corrosion of tungsten (●) and nickel (▲) in argon atmosphere.

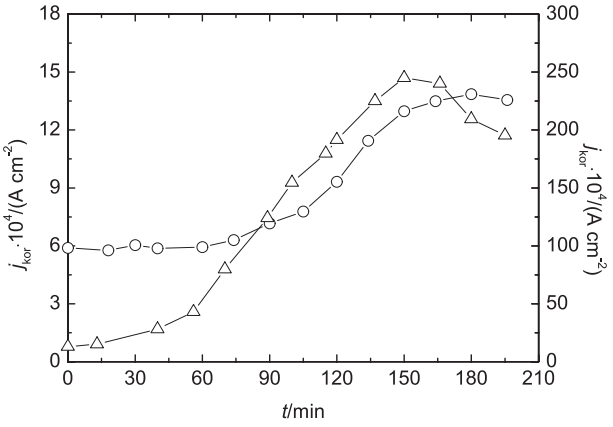


**Fig. 5.** Comparison of the corrosion current density obtained during corrosion of tungsten (○) and nickel (△; right axis) in air atmosphere.

In Fig. 6, comparison of the surface concentration of corrosion products obtained by chronopotentiometry and by digital simulation based on polarization resistance measurement is shown. Digital simulation was based on the approach presented in (Feldberg 1969), whereby a concentration of the corrosion products on sample surface (tungsten or nickel) was calculated (in simulation, diffusion coefficient $D = 5 \cdot 10^{-5}$ cm$^2$·s$^{-1}$ was considered). As can be seen from figure, the results of both methods are in a good agreement.

As follows from the time dependence of concentration of electroactive species during corrosion of nickel measured by chronopotentiometry (see Fig. 6), the corrosion rate decreases with time. That is also in a good agreement with the measurement of polarization resistance. Similar results were obtained also for tungsten.

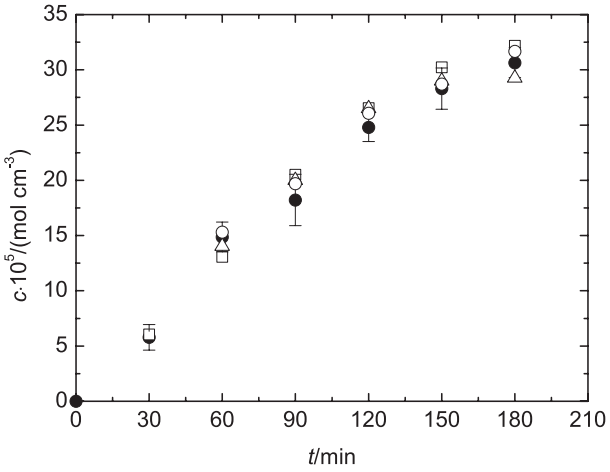


**Fig. 6.** Comparison of the surface concentration of corrosion products obtained by chronopotentiometry (●) and by digital simulation based on polarization resistance measurement (○, △, □).

In Fig. 7, concentration profiles of corrosion products obtained by digital simulation at different stages of nickel corrosion are shown. As can be seen from figure, a saturation level of corrosion products can be achieved near the surface of the matrix metal. Thus the soluble corrosion products can crystallize on the surface of the metal and thus partly inhibit corrosion. This is in agreement with the experimental results as mentioned above.

## Conclusion

It can be concluded that the presence of air (oxygen) in molten eutectic LiF-NaF-KF does not significantly influence the corrosion resistance of tungsten. On the other side, the presence of air (oxygen) rapidly decreases corrosion resistance of nickel. When comparing both metals, nickel is more resistant metal in the absence and tungsten in the presence of the air

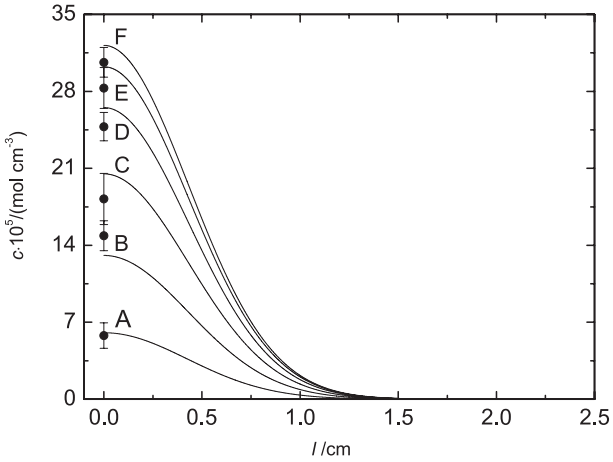


**Fig. 7.** Concentration profiles of corrosion products obtained by digital simulation at different stages of corrosion (30 min (A), 60 min (B), 90 min (C), 120 min (D), 150 min (E) and 180 min (F)). Points plotted at zero distance (metal surface) represent concentrations obtained by chronopotentiometry.

(oxygen). Rather high values of the overall change of thickness ($\Delta d$), evaluated for the final stage of corrosion measurements (see Table 2), indicate that any of the investigated metals cannot be itself used in the molten eutectic mixture LiF-NaF-KF.

*Acknowledgement*
*This work was supported by courtesy of the Slovak Grant Agency (VEGA 1/0588/11)*

## References

Bard AJ, Faulkner LR (2001) Electrochemical Methods. Fundamental and Applications, 2nd Ed., John Wiley & Sons Inc., New York, USA.

Büchel KH, Moretto H-H, Woditsch P (2000) Industrial Inorganic Chemistry, 2nd Ed., Wiley-VCH Verlag GmbH, Weinheim, Germany.

Feldberg SW (1969) Electroanalytical Chemistry 3: 199—296.

Joska L, Novák P (2001) Proceedings of "Koroze a její vliv na pevnost a životnost konstrukcí z oceli", Brno, 12.—13. 3. 2001, 61—66.

Koryta J (1980) Ionty, elektrody, membrány, Academia Praha.

Sand HJS (1901) Phil. Mag. 1: 45.

**Tab. 2.** Corrosion resistance of metals evaluated for the final stage of corrosion.

| Sample | Inert argon atmosphere | | Oxidation air atmosphere | |
|---|---|---|---|---|
| | $j_{cor}\cdot10^4/(A\cdot cm^{-2})$ | $\Delta d\cdot10^1/(cm\cdot r^{-1})$ | $j_{cor}\cdot10^4/(A\cdot cm^{-2})$ | $\Delta d\cdot10^1/(cm\cdot r^{-1})$ |
| tungsten | 10.450 | 8.1 | 12.970 | 9.4 |
| nickel | 3.497 | 2.5 | 188.600 | 144.3 |